

## Metallic mean-field stripes, incommensurability and chemical potential in cuprates

J. Lorenzana<sup>1</sup> and G. Seibold<sup>2</sup><sup>1</sup>Comision Nacional de Energía Atómica, Centro Atómico Bariloche and Instituto Balseiro, 8400 S.C. de Bariloche, Argentina<sup>2</sup>Institut für Physik, BTU Cottbus, P.O. Box 101344, 03013 Cottbus, Germany

(Dated: April 14, 2024)

We perform a systematic slave-boson mean-field analysis of the three-band model for cuprates with first-principle parameters. Contrary to widespread belief based on earlier mean-field computations low doping stripes have a linear density close to  $1/2$  added hole per lattice constant. We find a dimensional crossover from 1D to 2D at doping  $0.1$  followed by a breaking of particle-hole symmetry around doping  $1/8$  as doping increases. Our results explain in a simple way the behavior of the chemical potential, the magnetic incommensurability, and transport experiments as a function of doping. Bond centered and site-centered stripes become degenerate for small overdoping.

PACS numbers: 71.28.+d, 71.10.-w, 74.72.-h, 71.45.Jr

It is now a well established fact that doped holes in cuprates tend to self-organize in antiferromagnetic (AF) domain walls [1, 2, 3, 4, 5]. These quasi one-dimensional (1D) structures called stripes were predicted by mean-field theories [6, 7] inspired by the problem of solitons in conducting polymers [8].

In the superconducting systems observed stripes are parallel to the Cu-O bond (hereafter called vertical stripes) and for low doping have a linear filling fraction  $1/2$  of added holes per lattice constant ( $a = 1$ ). Unless a one-dimensional (1D) instability opens a gap at the Fermi level [9], half-filled ( $x = 1/2$ ) stripes are expected to be metallic. On the contrary mean-field theories predicted  $x = 1$  insulating stripes which led to an early rejection of stripes [10].

Here we perform a systematic analysis of slave-boson (SB) mean-field [11] solutions for a three-band Hubbard model as appropriate for the cuprates. Contrary to the early mean-field analysis we find that for low doping  $x$  in a material like  $\text{La}_{2-x}\text{Sr}_x\text{CuO}_4$  (LSCO) the most favorable stripes have indeed  $1/2$  (and are vertical) reconciling the mean-field picture with experiment. Small doping introduces more stripes at fixed  $d$  reducing the stripe distance  $d$  and explaining the observed behavior of the magnetic incommensurability  $\delta$  with  $\delta = 1/(2d)$  [1, 2, 3, 4, 5].

We find low doping stripes to be centered on oxygen, bridging two Cu sites, hereafter named bond centered (BC) stripes after the terminology of one-band models [12, 13] (see Fig. 1).

Significant interstripe overlap sets in at  $x = 0.1$  triggering a crossover from 1D behavior at low doping to 2D behavior at large doping. This does not affect the stability of stripes up to  $x = 1/8$  where a change of regime occurs. Further doping occurs at a fixed stripe distance  $d = 4$  and starts to grow. This explains the change of behavior observed in both the incommensurability [2, 3, 4, 5] and the chemical potential [14, 15] around doping  $x = 1/8$ . Furthermore for  $x < 1/8$  the chemical potential is at the center of an approximately particle-hole symmetric

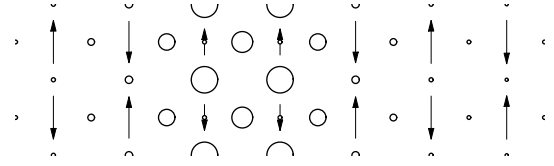


FIG. 1: BC vertical stripe with  $d = 7$  and  $x = 1/2$  ( $x = 1/2$ ). Sites with (without) arrows are Cu (O). The length of the arrows is proportional to the local magnetization on Cu (negligibly on O). The radius of the circle represents the excess charge respect to the AF state (0.09 holes for the largest one). The y axis is taken on the stripe direction (vertical). The picture repeats periodically in x and y directions.

band (Fig. 2) whereas for doping  $x > 1/8$  particle-hole symmetry is broken in good agreement with the picture deduced from transport experiments [6, 17]. Finally at  $x = 0.21$  BC stripes and site-centered (SC) stripes become degenerate suggesting a regime of soft lateral stripe fluctuations possibly relevant for superconductivity. This quasidegeneracy was found in more sophisticated treatments of (less realistic) one-band models [12, 13] however the ordering of the states was reversed [13].

One-band models can provide qualitative understanding but may miss subtle but important details specific for the cuprates. Therefore we use a three-band Hubbard model with a parameter set deduced from a first-principle LDA computation for LSCO [18]. We view our computation as the last stage of a first-principle computation and thus without free parameters. The largest repulsion  $U_d$  [18] is treated within a SB approach [11] fully equivalent to the Gutzwiller approximation and the other interactions are treated within the Hartree-Fock (HF) approximation (an equivalent formalism has been used in Ref. [19] for electron-doped cuprates). We solve the mean-field equations both in real and in momentum space. The real space computations are completely unrestricted [20] except for the spins which are assumed to be along the z axis.

Typically we minimize the energy in large clusters with

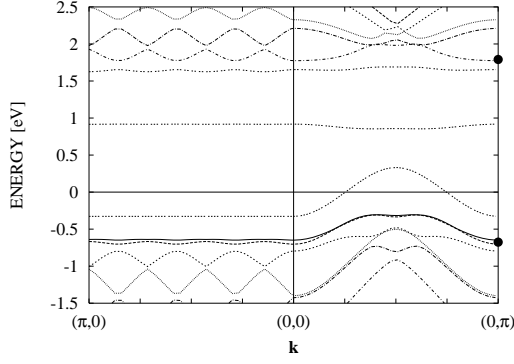


FIG. 2: Electron mean-field bands for the stripe of Fig. 1 measured from the chemical potential. Left (right) panel is in the direction perpendicular (parallel) to the stripe. We also plot the insulating charge transfer gap at momentum  $k = (0; 0)$  measured from the same reference energy (dots).

$N_s$  stripes ( $N_s = 2; 4$ ) of a maximum length  $L = 30$ . Depending on boundary conditions, size and filling, solutions with and without charge order in the stripe direction are obtained. In general due to the 1D character of stripes one expects that a 1D instability will develop in large systems at low doping rendering the system insulating even for  $\nu < 1$ . Indeed if superconductivity is suppressed by pulsed magnetic fields the system is insulating below a critical doping and a crossover temperature  $T_c$  [21]. In this work for simplicity we concentrate on the metallic state and restrict to solutions without charge order in the stripe direction. Since  $T_c$  is quite small compared with the typical electronic scales we can set the temperature to zero in our computations.

Fig. 1 depicts the typical charge and spin distribution for a BC vertical stripe. Added charge is accumulated in the antiphase boundary between the AF regions and mainly resides on oxygen sites.

In Fig. 2 we show the band structure for the electrons in an extended zone scheme. Two bands appear well inside the charge transfer gap. The upper one at  $\sim 0.9$  eV is more Cu like and quite flat (even in the stripe direction) whereas the lower one has substantial dispersion, is mainly O like, and crosses the Fermi level. Counting both in-gap bands the  $\nu = 1/2$  system corresponds to  $3/4$  hole ( $1/4$  electron) band filling. The gap between the bands is related to the magnetic character of the stripe. (It is absent in SC solutions with a non-magnetic core.) The electronic structure close to the chemical potential is well represented by a half-filled cosine like band, hereafter referred to as the active band.

The dispersion of the active band perpendicular to the stripe is quite flat indicating quasi 1D behavior. Small oscillations appear in this direction for  $d = 5$  which can be identified as a crossover interstripe distance from 1D to 2D behavior and corresponds to a crossover doping  $x = 0.1$  for  $\nu = 0.5$ .

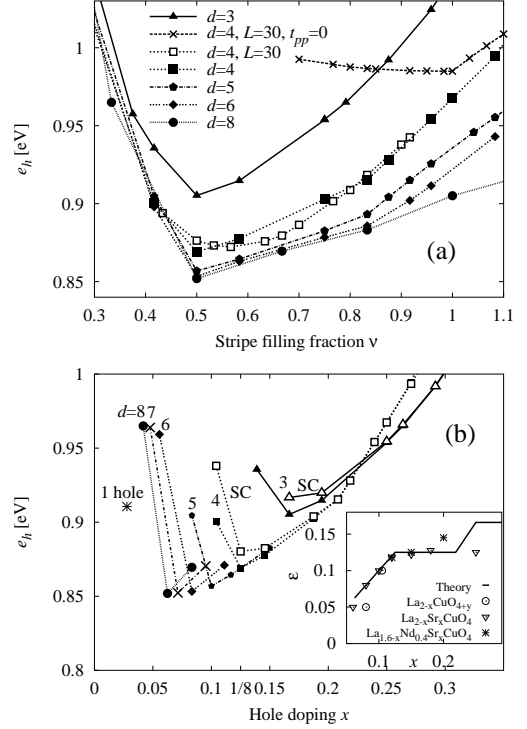


FIG. 3:  $e_h$  as a function of (a)  $\nu$  and (b)  $x$  for vertical BC stripes. Sizes are  $d = 12$  for  $d = 6$  and  $d = 24$  for  $d > 6$ . In (a) we also show the result for  $d = 30$  (open squares) and setting  $t_{pp} = 0$  shifted down by  $0.89$  eV (crosses). In (b) we also show the result for site-centered stripes (labeled SC, open symbols) for  $d = 3; 4$  and one self-trapped hole or "electronic polaron" at  $x = 1/36$ . The inset in (b) reports the incommensurability as obtained from the present calculation (line) compared with experimental data from Ref. [3].

The band structure in the stripe direction (right panel) is quite similar in all BC stripes solutions regardless of  $d$  which instead determines the periodicity in the perpendicular direction (left panel). Comparison with photoemission data requires matrix elements considerations and will be presented elsewhere. Here we notice that the Fermi surface crossing at vertical momentum  $k_y = \pi/4$  has been recently observed for  $d = 4$  stripes [22] and the portion of the active band in the direction perpendicular to the stripe correlates well with the flat bands observed in many cuprates around  $k = (\pi; 0)$  [23].

To evaluate the stability we compute the energy per added hole for  $N_h$  holes added to the system with  $N$   $\text{CuO}_2$  units,  $e_h = [E(N + N_h) - E(N)]/N_h$ . Here  $E(N + N_h) - E(N)$  is the total energy of the doped [undoped AF] solution. In Fig. 3 (a) we show  $e_h$  as a function of the filling fraction  $\nu = N_h/(N_s L)$  for BC vertical stripes. Each curve corresponds to a fixed  $d$ . The curves have a sharp minimum at  $\nu = 0.5$ . This is in contrast to early one-band [7, 9] and three-band mean-field computations [6] for which  $\nu = 1$  is the most favorable hole filling. We can reproduce this behavior by setting

artificially  $t_{pp} = 0$  in our parameter set (crosses). The difference in behavior can be understood by analyzing the band structure. In the case  $t_{pp} = 0$  the active band becomes as narrow as the 0.9eV band (Fig. 2) and a gap develops between the active band and the band immediately below instead of overlapping as in Fig. 2. This gap produces the cusp singularity at  $\nu = 1$  [Fig. 3 (a)] via the discontinuity in  $\partial E / \partial N$  which makes  $\nu = 1$  very stable. As  $t_{pp}$  is increased the gap closes, the cusp singularity disappears, and a minimum develops in the  $\nu < 1$  part of the curve. A simple model explains the formation of this minimum. Consider a flat density of states (DOS) of width  $W$  to estimate the kinetic energy of the active band and neglect interactions. In this approximation  $e_h = e_0 + W \nu / 2$  where  $e_0$  is the energy cost per unit length to create a domain wall in the undoped system ( $e_0 = J/2$  with  $J$  the superexchange constant). The optimum filling is given by  $\nu_{pt} = \min(2e_0/W; 1)$ . Increasing  $t_{pp}$  increases  $W$  without substantially affecting  $e_0$  and produces a local minimum for  $\nu < 1$ . The stability close to  $\nu = 1/2$  is further enhanced because the DOS of a 1D band is not flat but has a minimum at  $\nu = 1/2$ . For the same reason a gap produces a cusp in the energy, a minimum of the DOS enhances the local curvature of  $e_h$  vs.  $\nu$  and tends to shift the optimum filling closer to  $\nu = 1/2$ .

We have checked that for the most common parameter sets which contain  $t_{pp}$  [18] results are similar. However, as soon as  $t_{pp}$  is set to zero, as in Ref. [6], half-filled stripes become unstable in favor of filled ones.

The  $t_{pp} = 0$  result is in accord with HF computations in the simplest one-band model. Including a second-neighbor hopping ( $t^0$ ) we have found that partially filled stripes can be stabilized also in one-band models by a similar mechanism, which will be reported elsewhere.

Partially filled stripes were also found in the one-band Hubbard model with  $t^0 = 0$  in a much stronger correlation regime and going beyond a static mean-field [13]. In our case, because the active band is broad, correlations are less important and we expect that a static mean-field provides a good starting point.

Vertical stripes should be compared with other possible ground states. We find that within the present SB approach they are lower in energy than polaron solutions [24] [see Fig. 3 (b)] and diagonal stripes solutions (not shown). Very low nonsuperconducting dopings ( $x < 0.05$ ) were not explored in detail since we believe that a careful consideration of other effects is required in this case. Especially long-range order perpendicular to the planes favors bipolar configurations of stripes [12] and long-range Coulomb effects [25, 26] are expected to become important.

If one uses the HF approximation instead of SB the minimum also occurs at  $\nu = 1/2$  for BC vertical stripes. However a polaron lattice is the ground state in HF and diagonal stripes are lower in energy than vertical ones.

Thus the overall success of the present mean-field computation with respect to the earlier ones [6] is due to both a more accurate mean-field approximation (SB instead of HF) and a more accurate parameter set.

Further stabilization of the half-filled stripes can occur if due to many-body effects a gap or pseudogap tends to open at the commensurate filling  $\nu = 1/2$  [9]. Although we do not need this effect to explain  $\nu = 1/2$  it is quite possible that this produces a fine tuning for  $T < T_c$ . In this regard it is interesting to remark that the 'V' shape form of the curves in Fig. 3 (a) is due to the gap produced by the discretization of the levels in a finite system. For larger systems [see  $d = 4$  curve in Fig. 3 (a)] the cusp becomes rounded, however the minimum is still close to  $\nu = 1/2$ . One should be aware that the curves with the cusp are for already quite long stripes ( $L = 12$ ) and it is not clear whether stripes in real materials will be much longer. Thus finite size data could turn out to be more realistic than in finite size one.

For  $d > 4$  all curves coincide close to  $\nu = 0.5$  in Fig. 3 (a) whereas for  $d = 3, 4$  the curves are shifted up. This feature is due to the width of the domain wall of 4–5 lattice sites (see Fig. 1) which forces stripes to overlap leading to an increase of  $e_h$ .

In Fig. 3 (b) we show  $e_h$  for various values of the stripe separation  $d$  and as a function of doping  $x$  assuming each dopant introduces one hole. Since  $x = \nu d$  curves with larger  $d$  appear at lower concentration. The locus of the minimum of  $e_h$  as a function of doping in Fig. 3 (b) is expected to form a continuous curve in the thermodynamic limit by combining different  $d$  solutions in new solutions with larger periodicity. Up to  $x = 1/8$  the stripe filling is fixed at  $\nu = 0.5$  and consequently the density of stripes increases with doping. This explains the behavior of the incommensurability  $\nu = x/(2 - x)$  as seen in neutron scattering experiments in this doping range (inset of Fig. 3) [1, 2, 3, 4, 5]. For  $x > 1/8$  the right branch of the  $d = 4$  solution is more stable than the  $\nu = 0.5$  and  $d = 3$  solution due to the stripe overlap effect. Therefore the incommensurability remains locked at  $\nu = 1/8$  in good agreement with the change of behavior in  $\nu$  observed around  $x = 1/8$  [2, 3, 4, 5].

As doping increases further, BC stripes become degenerate with SC ones at  $x = 0.21$ . This suggests that as doping increases lateral fluctuations of the stripe will become soft and possibly mediate pairing between holes.

For doping  $x > 0.225$  we find the  $d = 3$  stripe ( $\nu = 1/6 \rightarrow 0.17$ ) to become the lowest energy solution with an initial filling fraction  $\nu = 0.675$ . Experimentally the situation is not clear.  $\nu = 1/6$  has been reported for  $YBa_2Cu_3O_{6+x}$  [5] (YBCO) but not for LSCO where it remains in the  $\nu = 1/8$  line up to  $x = 0.25$  (inset of Fig. 3). In  $La_{2-x-y}Nd_ySr_xCuO_4$  (LNSCO), where stripes are pinned by the low-temperature tetragonal lattice distortion, the incommensurability is substantially increased beyond  $\nu = 1/8$  at doping  $x = 0.2$  but without

reaching  $\gamma = 1/6$  [2].

It is possible that lateral stripe fluctuations become so strong at this doping range that an effectively isotropic state is reached [27]. Another possibility is that the  $d = 3$  phase is skipped due to phase separation among the  $d = 4$  phase and the overdoped Fermi liquid which for our parameters becomes the lowest energy solution close to  $x = 0.4$  (see Ref. [28] for a related scenario). Further theoretical and experimental work should be done to clarify this point. Especially being the system charged a careful analysis of phase separation is needed [26].

It has been recently emphasized [15] that there is a close connection between the doping dependent incommensurability as discussed above and the chemical potential in cuprates. In fact the chemical potential for the electrons can be related to  $e_h$  via:  $\mu = (e_h + x \frac{e_h}{x})$ . From Fig. 3(b) one can then deduce that  $\mu$  is approximately constant for  $x < 0.1$  and decreases for  $x > 0.1$  in qualitative agreement with the observed behavior [14, 15]. The rate of change of  $\mu$  with doping, being a high derivative of the energy, is very sensitive to finite size effects and, moreover, few experimental points are available in this doping range in order to allow for a precise comparison. A rough estimate indicates that the theoretical rate of change of  $\mu$  with doping for  $x > 1/8$  is approximately a factor of 2 larger than the experimental one [14, 15]. This may be due to phase separation among the  $d = 4$  stripe solution and the paramagnetic overdoped Fermi liquid as mentioned above.

We finally turn to the discussion of our calculation in light of recent measurements of the Hall coefficient  $R_H$  in  $\text{LNiSCO}$  [16] and  $\text{YBCO}$  [17]. In the former compound  $R_H$  displays an abrupt decrease below the charge-stripe ordering temperature  $T_0$  and for concentrations  $x = 1/8$ . It has convincingly been argued that quasi-1D transport is not enough to explain this anomaly and instead reflects a remarkable cancellation due to particle-hole symmetry in the stripe state [17, 29]. A partial suppression of  $R_H$  (and simultaneously the thermopower  $S$ ) below some temperature  $T_{\text{max}}$  has also been observed in  $\text{YBCO}$  up to oxygen contents corresponding to doping  $x = 1/8$  [17]. For distant stripes we indeed observe that the chemical potential crosses an approximately particle-hole symmetric band (see Fig. 2). Interstripe hopping becomes significant for  $x > 0.1$  however it does not break particle-hole symmetry. As discussed above the chemical potential shifts from the center of the band for  $x > 1/8$ , thus breaking particle-hole symmetry and consequently both  $R_H$  and  $S$  start to grow in modulus. Unfortunately the magnitude and even the sign of the transport coefficients cannot be predicted by a knowledge of the band structure alone. For example  $R_H$  for our Fermi surface (which turns out to be open) is determined by the unknown anisotropy of the scattering path length [30].

To conclude we have shown that, contrary to widespread believe, an appropriate mean-field theory of

stripe phases in cuprates is not in contradiction with experiments. Our theory explains in a simple way the change of behavior of several experimental quantities (incommensurability, chemical potential, transport coefficients) around the "magic" doping  $x = 1/8$ . Obviously the present stripes are static whereas those in real materials are dynamic unless pinned by a structural distortion. Many properties however will be largely independent of the dynamical or static character of the stripes. The energy for example is determined by short range correlations and is insensitive to the long-distant behavior. This is analogous to the problem of spin waves in a 1D antiferromagnet where the spin wave approximation gives a reasonable value for the energy although the system does not have true long-range order [31]. Since the properties we have discussed are mainly determined by the energetics we believe that the present mean-field theory is a good starting point for an understanding of the electronic structure of hole doped cuprates.

- 
- [1] J.M. Tranquada et al, Nature (London) 375, 561 (1995).
  - [2] J.M. Tranquada et al, Phys. Rev. Lett. 78, 338 (1997).
  - [3] K. Yamada et al, Phys. Rev. B 57, 6165 (1998).
  - [4] M. Arai et al, Phys. Rev. Lett. 83, 608 (1999).
  - [5] M. Arai et al, Int. J. Mod. Phys. B 14, 3312 (2000).
  - [6] J. Zaanen and O. Gunnarsson, Phys. Rev. B 40, 7391 (1989).
  - [7] D. Poilblanc and T.M. Rice, Phys. Rev. B 39, 9749 (1989). H.J. Schulz, Phys. Rev. Lett. 64, 1445 (1990).
  - [8] W.P. Su et al, Phys. Rev. Lett. 42, 1698 (1979).
  - [9] J. Zaanen and A.M. Oles, Ann. Phys. (Leipzig) 5, 224 (1996). M. Bosch et al, Phys. Rev. B 63, 092501 (2001).
  - [10] S.-W. Cheong et al, Phys. Rev. Lett. 67, 1791 (1991).
  - [11] G. Kotliar and A.E. Ruckenstein, Phys. Rev. Lett. 57, 1362 (1986).
  - [12] S.R. White and D.J. Scalapino, Phys. Rev. Lett. 80, 1272 (1989); 81, 3227 (1989).
  - [13] M. Fleck et al, Phys. Rev. Lett. 84, 4962 (2000).
  - [14] A. Ino et al, Phys. Rev. Lett. 79, 2101 (1997).
  - [15] N. Harima et al, Phys. Rev. B 64, R220507 (2001).
  - [16] T. Noda et al, Science 286, 265 (1999).
  - [17] Y. Wang and N.P. Ong, Proc. Natl. Acad. Sci. U.S.A. 98, 11091 (2001).
  - [18] A.K. McMahan et al, Phys. Rev. B 42, 6268 (1990) and references therein. We use  $\epsilon_{\text{Cu-O}} = 3.3\text{eV}$  for Cu-O onsite energy splitting,  $t_{\text{pd}} = 1.5\text{eV}$  ( $t_{\text{pp}} = 0.6\text{eV}$ ) for Cu-O ( $\text{O-O}$ ) hopping,  $U_{\text{d}} = 9.4\text{eV}$  ( $U_{\text{p}} = 4.7\text{eV}$ ) for onsite repulsion on Cu ( $\text{O}$ ) and  $U_{\text{pd}} = 0.8\text{eV}$  for Cu-O repulsion.
  - [19] A. Sadori and M. Grilli, Phys. Rev. Lett. 84, 5375 (2000).
  - [20] G. Seibold et al, Phys. Rev. B 57, 6937 (1998).
  - [21] G.S. Boebinger et al, Phys. Rev. Lett. 77, 5417 (1996).
  - [22] X.J. Zhou et al, Science 286, 268 (1999).
  - [23] D.M. King et al, Phys. Rev. Lett. 73, 3298 (1994).
  - [24] J. Lorenzana and L. Yu, Phys. Rev. Lett. 70, 861 (1993).
  - [25] U. Low et al, Phys. Rev. Lett. 72, 1918 (1994).
  - [26] J. Lorenzana et al, Europhys. Lett. 57, 704; Phys. Rev. B 64, 235127 (2001).
  - [27] S.A. Kivelson et al, Nature (London) 393, 550 (1998).

- [28] Y. J. Uemura, Solid State Commun. 120, 347 (2001).
- [29] P. Prelovsek et al., Phys. Rev. B 64, 052512 (2001).
- [30] N. P. Ong, Phys. Rev. B 43, 193 (1991).
- [31] P. W. Anderson, Phys. Rev. 86 (1952).